

## Search for $A \rightarrow Zh$ and $H \rightarrow ZA$ with the CMS detector

---

**Alexandre Mertens**<sup>\*†</sup>

*Université Catholique de Louvain*

*E-mail:* [alexandre.mertens@uclouvain.be](mailto:alexandre.mertens@uclouvain.be)

Extensions of the scalar sector predicts the existence of new scalar bosons. The searches for two interesting processes motivated simple extension of the scalar sector, the two-Higgs-doublet model, are reviewed. The first process is the production of a pseudoscalar decaying into a Z boson and a light Higgs and the second process is the production of a heavy Higgs scalar decaying into a pseudoscalar and a Z boson. While involving similar final states, these searches probe complementary parameter space. In particular the second is sensitive to the alignment limit in which the lightest scalar behaves as the standard model Higgs boson.

*38th International Conference on High Energy Physics  
3-10 August 2016  
Chicago, USA*

---

<sup>\*</sup>Speaker.

<sup>†</sup>On behalf of the CMS collaboration.

## 1. Extension of the scalar sector

A simple extension of the scalar sector, the Two-Higgs-Doublet-Model(2HDM), predicts the existence of five physical fields:  $h, H, H^\pm$  and  $A$ . In its simplest implementation, it is assumed that no CP-violation are present in the scalar sector and the lightest 2HDM scalar  $h$  corresponds to the observed 125 GeV boson. Three extra parameters are present in the model:

- $\tan\beta$  is the ratio between the vacuum expectation value of each of the Higgs doublets.
- $\alpha$  is the mixing angle of the two neutral even states, such that the coupling of the 2HDM light scalar is given by  $\frac{g_{hVV}}{g_{hVV}^{SM}} = \sin(\beta - \alpha)$ .
- $m_{12}$  is the soft- $\mathbb{Z}_2$  symmetry breaking parameter.

Four different types of couplings to the fermions are possible. The type-II, where one double couple to the up-type quark and the other couple to down-type quarks and charged leptons is studied here.

Several mass hierarchies are considered in this work and plotted on the left of Fig 1. On one hand, the MSSM-like hierarchy assumes a heavy pseudo-scalar degenerated in mass with the charged scalars. On the other hand, an inverted mass hierarchy(im2HDM) [1] is also possible and predicts the  $H$  to be the heaviest neutral and degenerated in mass with the charged Higgs bosons. In this case, the pseudoscalar mass is not bounded by the discovered scalar mass and can therefore be lower than 125 GeV.

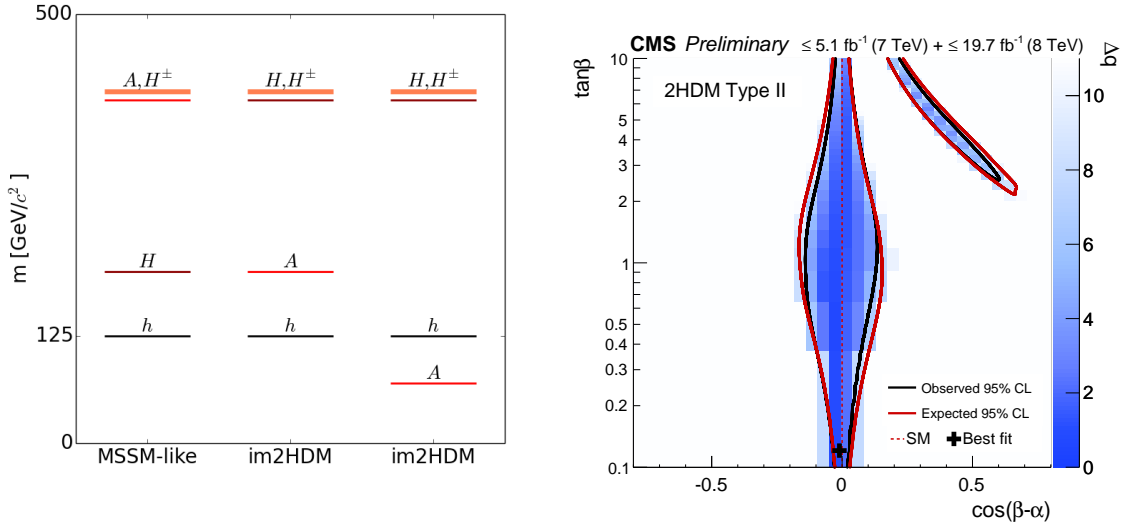


**Figure 1:** Left: Three different mass hierarchies for the CP conserving 2HDM. The most left correspond to the MSSM scalar sector while the two other are inverted hierarchies, where the pseudoscalar is lighter than the scalar triplet. Right: Excluded region in the 2D  $\cos(\beta - \alpha)$ - $\tan\beta$  plane from the coupling measurements of the 125 GeV scalar [2].

The measurement of the couplings of the 125 GeV particle brings indirect constraints on  $\cos(\beta - \alpha)$  and  $\tan\beta$  and the excluded region is plotted on the right of the Fig 1. The align-

ment limit defined as the limit where  $\cos(\beta - \alpha) \approx 0$  is favored. It corresponds to the region where the light 2HDM boson couplings are equal to the standard model case.

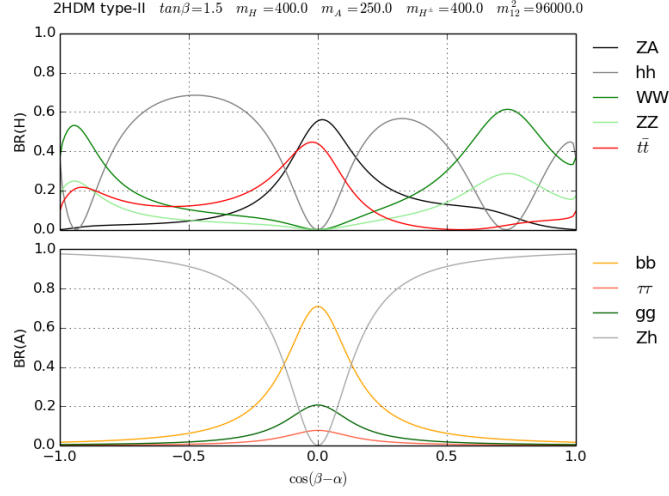


**Figure 2:** Branching fractions of the 2HDM heavy scalar boson (top) and pseudo-scalar boson (bottom) as a function of  $\cos(\beta - \alpha)$  for a particular parameter choice.

The branching fractions of the scalar and pseudoscalar are plotted on Fig 2 where the parameter choice is made to illustrate the many allowed decays. The search for a pseudoscalar decaying into a Z boson and a light scalar, sensitive to a vast region in the parameter space, is presented in Sec 2 and the alignment limit motivated search for a heavy scalar decaying to a Z boson and a pseudo scalar is discussed in Sec 3.

## 2. Search for $A \rightarrow Zh$

This process has been studied with the CMS detector in many different final states. It includes searches for  $h \rightarrow \tau\tau$  [3] and  $h \rightarrow b\bar{b}$  [4] performed with the data from the first run of the LHC.

In both analyses, a Z boson candidate is reconstructed by requiring a pair of two opposite sign, same flavor and isolated electrons (muons) with  $|\eta| < 2.5(2.4)$  and  $p_T > 20$  and 10 GeV for the leading and sub-leading electron (muon) respectively.

### 2.1 The $ll\tau\tau$ channel

In the  $ll\tau\tau$  channel, eight final states have been considered. The two di-lepton Z decay to  $ee$  and  $\mu\mu$  with a mass required to be between 60 and 120 GeV and four different  $\tau\tau$  decays:  $\mu\tau_h, e\tau_h, \tau_h\tau_h, e\mu$ . After several additional cuts performed to reduce the main backgrounds, the A boson mass is reconstructed from the Z boson candidate four vectors information and from the h candidate four vector information reconstructed using a dedicated algorithm called SVFIT [5] which combines information from the  $\tau$  leptons and from the  $E_T^{miss}$  in a likelihood estimator.

In this search, no evidence of signal is observed in the invariant mass spectra and therefore upper limits on the cross section are set using a binned maximum likelihood fit. The upper limits at 95% CL on the cross section times branching fraction for the eight final states combined is plotted

on the left of Fig 3 for a pseudoscalar mass between 200 and 350. These mass values are close to the sum of the Z and the Higgs boson mass and to twice the top mass respectively.

## 2.2 The $llb\bar{b}$ final state

In addition to the Z candidate with an invariant mass between 75 and 105 GeV, at least two b-tagged jets are required with  $p_T > 20$  GeV, within  $|\eta| < 2.4$  and  $90 < m_{bb} < 140$  GeV. A kinematic fit is used and improves the four body invariant mass resolution by constraining the di-jet mass to be equal to 125 GeV. The discrimination of the signal from the background is performed with three different boosted decision trees trained separately for three different mass regions (low :  $m_A = 225, 250$  and  $275$  GeV, intermediate :  $m_A = 300, 325$  and  $350$  GeV and high mass :  $m_A = 400, 500$  and  $600$  GeV).

The result is obtained from a combined signal and background fit to the two dimensional ( $m_{llbb}$ , BDT output) distribution and no deviations from the background expectation have been observed. Therefore, 95% CL upper limits on the cross section times branching fraction are plotted on right part of Fig 3 as a function of the A boson mass in the narrow width approximation and in Fig 5 as a function of  $\tan\beta$  and  $\cos(\beta - \alpha)$ , for  $m_A = 300$  GeV.

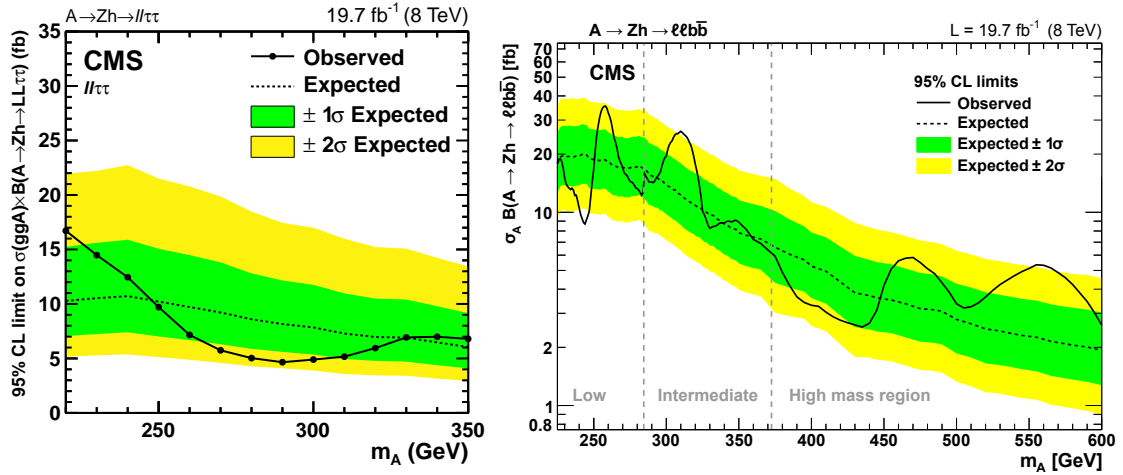


**Figure 3:** Left: Upper limits at 95% CL on cross section times branching fraction on  $A \rightarrow Zh \rightarrow LL\tau\tau$  for all  $ll\tau\tau$  final states combined. Right: Observed and expected 95% CL upper limit on  $\sigma \times \mathcal{B}(A \rightarrow Zh \rightarrow llb\bar{b})$  as a function of  $m_A$  in the narrow-width approximation.

## 3. Search for $H \rightarrow ZA$

Two final states are considered, the  $ll\tau\tau$  and the  $llb\bar{b}$  [6] and both analyses are sensitive also to the  $A \rightarrow ZH$  process from the MSSM-like hierarchy since no spin-dependent variables are used. This section focus on the  $llb\bar{b}$  decay since it is currently the most sensitive thanks to the high branching fraction.

Events with two isolated, same flavor and opposite sign leptons are selected. Two b-tagged jets are then required and only events with a small missing transverse energy significance are selected. The strategy is then to perform rectangular cuts in the plane ( $m_{bb}, m_{llbb}$ ) around each tested mass

pair and search for excesses of events compared to the background expectation. The width of the rectangular cut is taken to be three times the experimental resolution, taken as 15% of the reconstructed mass in both dimension. To cover the full 2D map, the distance between a tested mass pair and the next is taken to be one third of the rectangle width.

The analysis has been performed with 2012 data at 8 TeV and with 2015 data at 13 TeV in the center of mass with only little differences [7]. In both analyses, no significant excess compared to the expected background have been observed. At 8 TeV, the limit on the cross section has been combined with the  $l\tau\tau$  channel and plotted on the left of the Fig 4 as a function of  $m_A$  and  $m_H$ . At 13 TeV, the limits on the cross section were tested for  $m_H = 300, 500$  and  $800$  GeV, the second is plotted on the right part of the Fig 4.

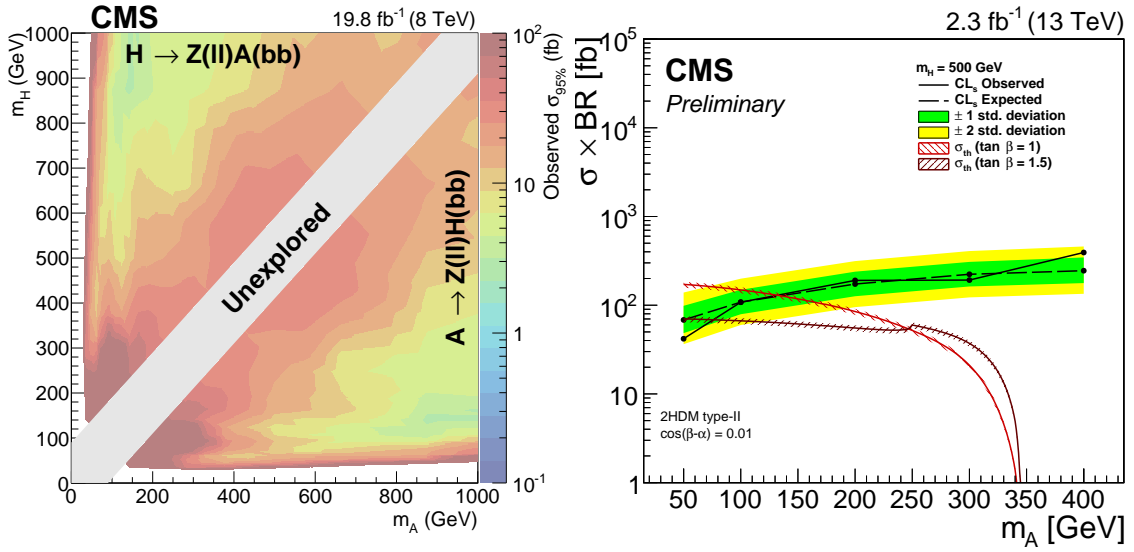


**Figure 4:** Left: Observed 95% CL upper limits on  $\sigma(H/A \rightarrow ZA/H \rightarrow llb\bar{b})$  as a function of  $m_A$  and  $m_H$ . Right: Limit on the  $\sigma \times BR(H \rightarrow ZA) \times BR(Z \rightarrow ll) \times BR(A \rightarrow b\bar{b})$  for  $m_H = 300, 500, 800$  GeV. The predicted production cross section are also shown for different values of  $\tan\beta$ .

The exclusion limit as a function of  $\tan\beta$  and  $\cos(\beta - \alpha)$  is plotted on the right of the Fig 5. This analysis is sensitive to the alignment limit for  $\tan\beta \approx 1$  and a part of the parameter space has been excluded already with the 2012 data.

#### 4. Conclusion

Extensions of the scalar sector, such as the 2HDM predicts the existence of extra scalars. The searches for two interesting processes motivated by the 2HDM are reviewed. The first process is the production of a pseudoscalar decaying into a Z boson and a light Higgs in the  $l\tau\tau$  and  $llb\bar{b}$  final states. The second process is the production of a heavy Higgs scalar decaying into a pseudoscalar and a Z boson.

Since no deviation from the expected background have been observed, upper limits on cross section have been derived for both processes. The two type of searches show a very important complementarity: the first search is mostly sensitive to parameter space where  $\cos(\beta - \alpha)$  is different from 0, while the second is sensitive in the alignment limit.

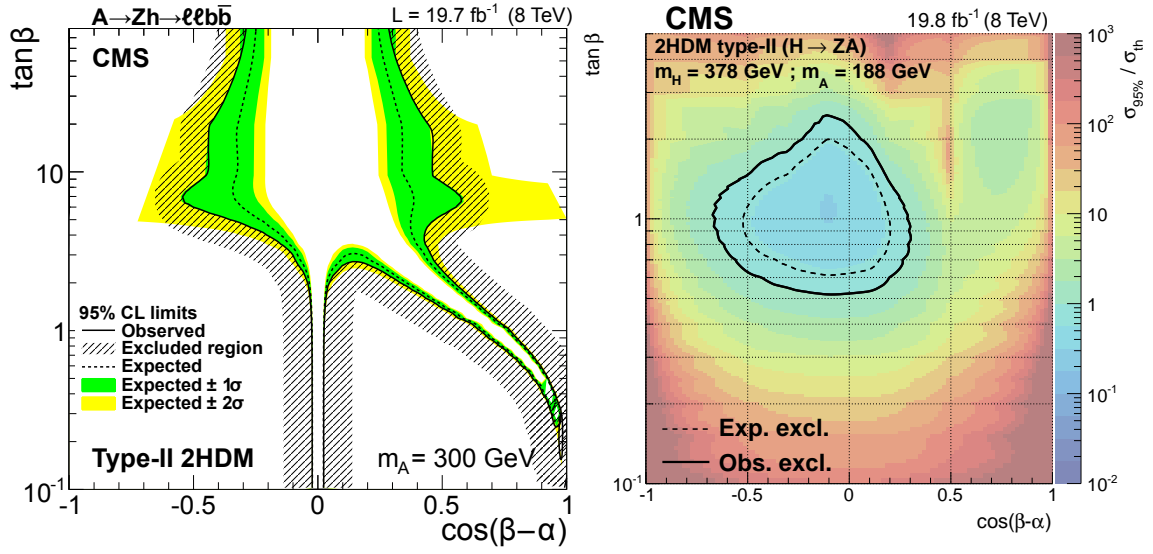


**Figure 5:** Left: Observed and expected exclusion limit for Type-II 2HDM, as a function of  $\tan\beta$  and  $\cos(\beta - \alpha)$ , for  $m_A = 300$  GeV. Right: Observed limits on the signal strength  $\mu = \sigma_{95\%}/\sigma_{th}$  for the 2HDM benchmark after combining results from  $llb\bar{b}$  and  $ll\tau\tau$  final states. Limits are shown in the 2HDM parameters  $\cos(\beta - \alpha)$  and  $\tan\beta$  for the signal masses of  $m_H = 378$  GeV and  $m_A = 188$  GeV. The dashed contour shows the region expected to be excluded. The solid contour shows the region excluded by the data.

## References

- [1] S. de Visscher, J. M. Gerard, M. Herquet, V. Lemaître and F. Maltoni, JHEP **0908**, 042 (2009) doi:10.1088/1126-6708/2009/08/042 [arXiv:0904.0705 [hep-ph]].
- [2] CMS Collaboration [CMS Collaboration], CMS-PAS-HIG-16-007.
- [3] V. Khachatryan *et al.* [CMS Collaboration], Phys. Lett. B **755**, 217 (2016) doi:10.1016/j.physletb.2016.01.056 [arXiv:1510.01181 [hep-ex]].
- [4] V. Khachatryan *et al.* [CMS Collaboration], Phys. Lett. B **748**, 221 (2015) doi:10.1016/j.physletb.2015.07.010 [arXiv:1504.04710 [hep-ex]].
- [5] L. Bianchini, J. Conway, E. K. Friis and C. Veelken, J. Phys. Conf. Ser. **513**, 022035 (2014). doi:10.1088/1742-6596/513/2/022035
- [6] V. Khachatryan *et al.* [CMS Collaboration], Phys. Lett. B **759**, 369 (2016) doi:10.1016/j.physletb.2016.05.087 [arXiv:1603.02991 [hep-ex]].
- [7] CMS Collaboration [CMS Collaboration], CMS-PAS-HIG-16-010.